LBL-27943
Preprint

Lawrence Berkeley Laboratory
UNIVERSITY OF CALIFORNIA

Submitted to Physical Review C

Heavy Actinide Production from the Interactions of ^{40}Ar with ^{248}Cm

J.D. Leyba, R.A. Henderson, H.L. Hall, C.M. Gannett, R.B. Chadwick, K.R. Czerwinski, B.A. Kadkhodayan, S.A. Kreek, G.R. Haynes, K.E. Gregorich, D.M. Lee, M.J. Nurmia, and D.C. Hoffman

October 1989

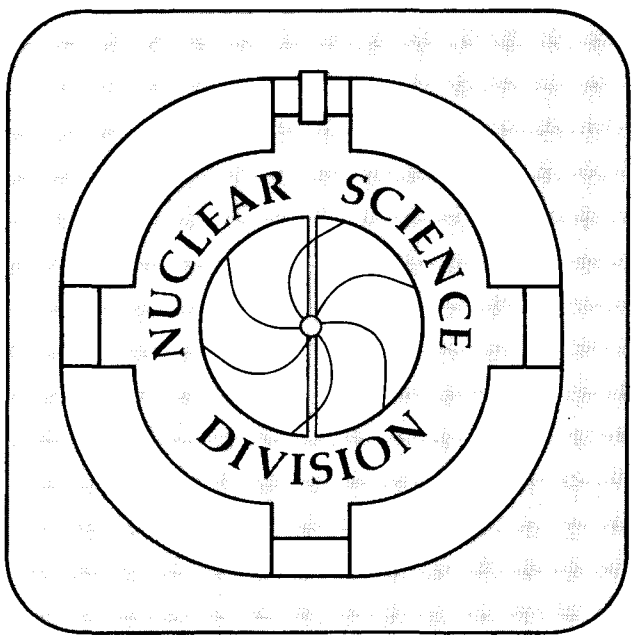

Prepared for the U.S. Department of Energy under Contract Number DE-AC03-76SF00098.

DISCLAIMER

LBL-27943

Heavy Actinide Production From The Interactions Of ^{40}Ar With ^{248}Cm

J.D. Leyba, R.A. Henderson, H.L. Hall, C.M. Gannett*, R.B. Chadwick, K.R. Czerwinski, B.A. Kadkhodayan, S.A. Kreek, G.R. Haynes+, K.E. Gregorich, D.M. Lee, M.J. Nurmia, and D.C. Hoffman

Department of Chemistry, University of California, Berkeley, CA 94720

and

Nuclear Science Division, Lawrence Berkeley Laboratory, University of California, Berkeley, CA 94720.

*Forensics Division, Orange County Sheriff's Department, 601 North Ross, Santa Ana, CA 92701.

+University of Illinois, Urbana, IL 61801.

October 1989

This work supported in part by the Director, Office of Energy Research, Division of Nuclear Physics of the Office of High Energy and Nuclear Physics of the U.S. Department of Energy under Contract No. DE-AC03-76SF00098.

Heavy Actinide Production From The Interactions Of ^{40}Ar With ^{248}Cm

J.D. Leyba, R.A. Henderson, H.L. Hall, C.M. Gannett*, R.B. Chadwick, K.R. Czerwinski, B.A. Kadkhodayan, S.A. Kreek, G.R. Haynes+, K.E. Gregorich, D.M. Lee, M.J. Nurmia, and D.C. Hoffman

Department of Chemistry, University of California, Berkeley, CA 94720

and

Nuclear Science Division, Lawrence Berkeley Laboratory, University of California, Berkeley, CA 94720.

*Forensics Division, Orange County Sheriff's Department, 601 North Ross, Santa Ana, CA 92701.

+University of Illinois, Urbana, IL 61801.

ABSTRACT

Excitation functions have been measured for isotopes of Bk, Cf, Es, and Fm produced from the interactions of 207- to 286-MeV ^{40}Ar ions with ^{248}Cm. The measured isotopic distributions were found to be essentially symmetric with full-widths-at-half-maximum between 2.0 and 3.5 mass units. These results are comparable to those obtained in previous studies using $^{40,44,48}Ca$ with ^{248}Cm. The maxima of the isotopic distributions from the ^{40}Ar-^{248}Cm system show shifts, to both heavier and lighter mass numbers, of 0 to 2 mass units relative to the corresponding maxima of the isotopic distributions from the $^{40,44,48}Ca$-^{248}Cm.

NUCLEAR REACTIONS $^{248}Cm(^{40}Ar,X)$, $E(^{40}Ar)$ = 207, 225, 245, 266 and 286 MeV; Excitation functions and isotopic distributions were measured for Z = 97-100.

This work supported in part by the Director, Office of Energy Research, Division of Nuclear Physics of the Office of High Energy and Nuclear Physics of the U.S. Department of Energy under Contract No. DE-AC03-76SF00098.

I. INTRODUCTION

Transfer reactions, discovered by Kaufman and Wolfgang in the early 1960's,[1] are a group of nuclear interactions in which a small number of nucleons are exchanged between two nuclei. Complete fusion does not take place since these reactions occur at rather large impact parameters. The projectile-like product can carry off a large fraction of the kinetic energy and angular momentum, thus leaving the target-like product "cold." Because of this fact, transfer reactions involving actinide targets and heavy ions have been found to be useful for producing neutron-rich actinide products with little excitation energy.

Since the availability of large quantities of ^{248}Cm, this nuclide has become a popular target for many different transfer reaction studies. ^{248}Cm is an attractive target material for many reasons including high neutron to proton ratio, long half life, and its availability in nearly isotopically pure milligram quantities.[2] Actinide production studies using ^{248}Cm with various projectiles ranging from ^{13}C to ^{238}U have been performed in order to gain some insight into the reaction mechanism(s) involved.[3-11] In an attempt to study the influence of an additional pair of neutrons in the projectile on the actinide production cross sections, Lee et al.[6] bombarded ^{248}Cm with the projectile pairs $^{16,18}O$ and $^{20,22}Ne$. It was found that as the number of neutrons in the projectile was increased by 2, the corresponding maxima of the mass-yield curves for the above target elements ($Z_{product} > Z_{target}$) were increased by about 2 mass units. Hence, the neutron-rich projectile of each pair enhanced the neutron rich actinide production.

Experiments using the projectiles $^{40,48}Ca$ were performed to see what the effect of the 8 neutron excess of ^{48}Ca relative to ^{40}Ca would have on the final actinide production distribution.[3] Shifts to heavier masses of only 2-3 units in the mass-yield curves for the elements Bk, Cf, Es, and Fm were observed between the ^{40}Ca and ^{48}Ca systems. The 8 neutron excess of ^{48}Ca relative to ^{40}Ca did not increase the maxima of the isotopic distributions by 8 mass units and hence had only a partial effect on the final isotopic distributions of the above target products.

In order to further study the effect of the neutron number of the projectile on the final isotopic distributions in reactions involving ^{248}Cm in more detail, ^{44}Ca was employed as a projectile.[4] For this system, increases in the mass number of the maxima of the isotopic distributions of only 0-2 mass units

relative to the maxima for ^{40}Ca reactions were observed. All of the maxima from the ^{44}Ca system fell between the corresponding maxima from the ^{40}Ca and ^{48}Ca systems.

Welch et al.[7] observed in the $^{129,132,136}Xe$ systems that the peaks in the cross section distributions for Fm, Bk, and Pu shifted to higher mass numbers as the projectile mass number increased. Shifts in the Cf and Es peaks could not be verified because of insufficient data. However, production cross sections for the most neutron-rich above target nuclides were found to be independent of the projectile mass.

As part of our effort to obtain a better understanding of binary transfer reactions we are systematically studying actinide production cross sections from the interactions of heavy ions with actinide targets. In the present study ^{40}Ar was used as the projectile with a ^{248}Cm target. ^{40}Ar was chosen because it has a neutron to proton ratio (N/Z) of 1.22 which lies between the ^{48}Ca and ^{40}Ca neutron to proton ratios of 1.40 and 1.00 respectively, and it has the same mass number as ^{40}Ca. In addition, ^{40}Ar has a neutron to proton ratio that is quite similar to the 1.20 ratio of ^{44}Ca. The neutron to proton ratios for various projectiles are shown in Table I.

II. EXPERIMENTAL

All of the irradiations of ^{248}Cm were performed at the 88-Inch Cyclotron at the Lawrence Berkeley Laboratory with 207-, 225-, 245-, 266-, and 286-MeV ^{40}Ar ions. All energies have been corrected for the appropriate energy loss in our target system and represent the average energy of the ions in the target in the laboratory frame of reference. The ^{40}Ar beam, after being collimated by a water cooled graphite collimator, passed through a 1.8 mg/cm^2 Havar isolation foil, 0.2 mg/cm^2 nitrogen cooling gas, 2.75 mg/cm^2 Be backing foil and finally the target material. The target consisted of 0.491 mg/cm^2 ^{248}Cm (96.5% ^{248}Cm; 3.5% ^{246}Cm) in the form of Cm_2O_3 electrodeposited on the Be backing. The recoiling reaction products were stopped in 12.26 mg/cm^2 Au catcher foils. A schematic diagram of the target system is shown in Fig. 1.

The Au catcher foils were dissolved in approximately 0.25 ml of aqua regia containing a known amount of ^{241}Am tracer. An ether extraction was performed on this solution to remove about 95% of the gold.[12] The aqueous phase was passed through a 3-mm

diameter by 10-mm long column of Bio Rad AG-1, X-8 anion exchange resin in 12M HCl. The remaining gold was adsorbed on the resin while the trivalent actinides passed through. This effluent was evaporated to dryness and fumed twice with concentrated perchloric acid to remove any organic residue. The remaining activity was picked up in 0.5 M HCl and sorbed on a 2-mm diameter by 50-mm long column of Dowex-50, X-12 cation exchange resin (7-10 μm) kept at 80° C. The trivalent actinides were eluted from the column in separate fractions using 0.5 M ammonium alpha-hydroxyisobutyrate (α-HIB) at a pH of 3.80. The chemical yields for the trivalent actinides were determined from the ^{241}Am tracer. The average time for the chemical separations was 2.0 hours. A chemistry flowchart is presented in Figure 2.

The isolated Bk fractions were counted using Ge(Li) or high-purity Ge gamma-ray spectrometer systems. The Cf and Fm fractions were assayed with a fission-alpha spectrometer system utilizing Si(Au) surface barrier detectors. The Es samples were assayed for gamma, alpha and spontaneous fission activities simultaneously by mounting the isolated samples in a vacuum chamber which contained a Si(Au) surface barrier detector. This chamber was then positioned next to a Ge(Li) gamma-ray detector. Samples were continuously counted for 4 weeks after the end of bombardment and then at appropriate intervals so that unambiguous nuclide identification could be established.

Alpha spectra were integrated using a simple computer code. Gamma-ray spectra were analyzed with the SAMPO[13] code. Decay curve analyses were performed with the EXFIT[14] and CLSQ[15] computer codes. The activities at the end of bombardment were extrapolated from the decay curve fits. Activities at end of bombardment, detector efficiencies, nuclide half-lives, chemical yields, number of target atoms per square centimeter, and the beam intensities as a function of time were used to determine the cross sections for the various transfer products. In each experiment it was assumed that 100% of the transfer products of interest recoiled out of the target and into the Au catcher foil. A standard deviation of 12%, as described before,[6] on the calculated absolute cross sections is estimated. This is in addition to the statistical standard deviations in the data and decay curve analyses.

III. RESULTS AND DISCUSSION

The cross sections obtained in these experiments are summarized in Table II. Appropriate corrections to the measured activities of the daughters have been made for the contributions from the decay of the parent nuclides. Since the absolute abundance of the 217.6-keV gamma-ray is not known, the cross sections presented here for ^{244}Bk are lower limits based upon the assumption that the 217.6-keV line has an abundance of 100%. The cross sections for ^{250}Es are the sum of the cross sections for the 6^+ (8.6 h) and 1^- (2.1 h) isomers.

A. Excitation functions

Excitation functions for the production of above target elements for the ^{40}Ar system are shown in Figs. 3-6. Theoretically, for the capture of charged particles, the cross section should increase with increasing bombarding energy of the projectile since the maximum impact parameter, b_m, for such processes goes as

$$b_m = R(1 - V_C/\varepsilon)^{1/2}$$

where R is the interaction radius, V_C is the Coulomb barrier between the target and the projectile, and ε is the kinetic energy of the projectile. This function increases with ε until it asymptotically approaches R at high ε. However, as more energy is deposited in the system, the probability for particle emission and/or fission increases. Hence, at some higher energy the decrease in yield due to particle emission and fission should be greater than the increase resulting from the higher bombarding energy. As a result the net production cross section for a given nuclide decreases.

1. Excitation energies

Excitation energies at the Coulomb barrier for the various target-like fragments and projectile-like fragments have been calculated for both the ^{40}Ar and ^{44}Ca systems and are shown in Tables III and IV respectively. These excitation energies are based upon the Coulomb barriers in the entrance and exit channels and ground state Q values.[16] For those reactions with negative excitation energies, a maximum in the excitation function should

be reached at some energy above the Coulomb barrier and then a decrease should be observed at higher energies. Reaction channels with positive reaction energies comparable to the neutron binding energies or the fission barriers should have excitation functions which are near their maxima at the Coulomb barrier and decrease with increasing projectile energy.

2. Excitation functions for Bk isotopes

Excitation functions for the Bk isotopes 244, 245, 246, 248m, and 250 are shown in Fig. 3. The shapes of the functions are consistent with the calculated excitation energies. It is expected that the production cross section will be highest for the isotope requiring the exchange of the fewest nucleons, provided E_x is positive, but not large enough to cause fission or neutron emission. Based on the data in Table III, ^{249}Bk should have the largest production cross section since it can be formed by the transfer of the fewest nucleons, only one proton, and E_x is positive. ^{249}Bk was not measured since it is used as a tracer in our laboratory; therefore, an accurate cross section for this nuclide could not be determined. ^{248m}Bk has the highest production cross section with ^{250}Bk having the next highest, followed by ^{246}Bk, ^{245}Bk and finally ^{244}Bk. All of the Bk isotopes require the transfer of 1 proton from the projectile to the target along with the exchange of various numbers of neutrons. For example ^{248m}Bk requires the exchange of only 1 neutron whereas ^{244}Bk requires a 5 neutron transfer.

3. Excitation functions for Cf isotopes

The excitation functions measured for the Cf isotopes are shown in Fig. 4. These are all similar in shape showing an increase by a factor of 2.5 when the bombarding energy is increased by 18 MeV, then they level off for the next 41 MeV and finally decrease by a factor of 2.5 over the next 20 MeV. The highest cross sections occur for ^{250}Cf which results from the transfer of only 2 nucleons (2 protons), the fewest possible, and the lowest cross section occurs for ^{254}Cf which results from the transfer of 6 nucleons (2 protons and 4 neutrons).

4. Excitation functions for Es isotopes

Excitation functions for the Es isotopes 250-255 are plotted in Fig. 5. Again the shapes of the functions are consistent with

the calculated excitation energies, and again the highest cross section occurs for ^{251}Es resulting from the transfer of the fewest number of nucleons, in this case 3 protons. A decrease in the production cross sections is seen as the number of nucleons transferred increases.

5. Excitation functions for Fm isotope

Excitation functions for isotopes of Fm are shown in Fig. 6. The curves are all similar in shape and are consistent with their calculated positive excitation energies. The fewest number of nucleons which can be transferred to make a Fm isotope is 4, and indeed, ^{252}Fm is the highest cross section. The cross sections decrease as the number of nucleons transferred increases with ^{252}Fm having the largest cross section and ^{255}Fm having the smallest.

B. Calculation of F_t

An estimate of the fraction, F_t, of the projectile kinetic energy transformed into target-like fragment excitation energy was attempted using the equation

$$F_t = (E_{f,n} - E_x)/(E_M - E_B)$$

where $E_{f,n}$ is the height of the fission[17,18] barrier or the neutron binding energy in MeV whichever is lower, E_x is the excitation energy described earlier, E_M is the maximum in the experimental excitation functions, and E_B is the calculated Coulomb barrier. This formula assumes that the maximum in the excitation function occurs when the product excitation energy is comparable to the fission barrier or neutron binding energy. F_t's for the ^{40}Ar system are shown in Table V and for the ^{44}Ca system in Table VI[19]. It should be noted that the Cf excitation functions are relatively flat; therefore, the E_m's for these isotopes were difficult to locate thus affecting the F_t values. The F_t's range in value from 0.02 to 0.34, with average values of 0.16, 0.14, 0.18, and 0.19 for the Bk, Cf, Es, and Fm isotopes respectively for the ^{40}Ar system. F_t values for the ^{44}Ca system were found to be approximately 0.01 to 0.63 with average values of $\leq$0.03, 0.22, 0.24, and 0.14 for the Bk, Cf, Es, and Fm isotopes respectively. As can be seen, the average F_t's generally increase in going from Bk to Fm. There are, however, a couple of exceptions. In the ^{40}Ar system, Cf does not follow the

trend, whereas in the ^{44}Ca system Fm is the exception. E_t, the fraction of energy transferred assuming energy transfer is proportional to mass transfer, is also shown in Tables V and VI. E_t, which can appear as excitation energy of the heavy product, was calculated using the formula

$$E_t = M/A$$

where M is the number of nucleons transferred and A is the mass number of the projectile. No correlation was found between F_t and E_t for a given nuclide; however, in general, E_t is less than F_t indicating that the fraction of energy transferred is greater than the fraction of mass transferred. Lee et al. also found this to be the case for the ^{18}O-^{248}Cm and ^{18}O-^{249}Cf systems[9] where the average F_t value was approximately 0.5. The calculated F_t values for the ^{40}Ar system are expected to be smaller than those from the ^{18}O systems if the energy transferred is proportional to the fraction of mass transferred.

C. Isotopic distributions

1. General features

Isotopic distributions for Bk, Cf, Es, and Fm from the interactions of 245-MeV ^{40}Ar ions with ^{248}Cm are plotted in Fig. 7. The lines connecting the experimental points are included only to aid the eye. The maxima of the mass-yield curves for the ^{40}Ar system occur at ^{248m}Bk, ^{250}Cf, ^{251}Es, and less than or equal to ^{252}Fm, exactly the same as for the ^{44}Ca system (See Fig. 8). Since the cross sections for the neutron-deficient Fm isotopes were not measured, the peaks of the mass distributions for the Fm isotopes of the ^{40}Ar and ^{44}Ca systems cannot be located with certainty. However it can be said that the peaks occur at a mass number of 252 or less. For both the ^{40}Ar and ^{44}Ca systems, the measured isotopic distributions are essentially symmetric with full-widths at half-maximum (FWHM) of 1.5-3.25 mass units for the ^{40}Ar system and 2.0-3.5 mass units for the ^{44}Ca system. For the ^{40}Ca system, the maxima of the mass-yield curves occur at ^{247}Bk, ^{248}Cf, ^{248}Es, and ^{250}Fm. The shapes of the isotopic distributions from this system are all very similar with FWHM's of about 2.5 mass numbers. Values of 2.5 and 3.0 mass units have been reported previously for the ^{48}Ca system[3] and the ^{238}U system[8] respectively. The final isotopic distributions for Bk, Cf, Es, and Fm produced from the interactions of various heavy

ions (HI) on ^{248}Cm are shown in Figs. 9-12.

2. Comparison of the ^{40}Ar and ^{44}Ca systems

The peak production cross section for the Bk mass-yield curve is about thirty percent larger for the ^{40}Ar system than for the ^{44}Ca system. However, the widths of the peaks are essentially the same. In addition, the cross sections for the neutron-deficient Bk isotopes ($^{244,245}Bk$) are about the same for the two systems but the ^{40}Ar gives higher yields for the neutron-rich Bk isotopes. The mass-yield curves for the Cf isotopes of the 2 systems are almost identical both in magnitude and in width. However, a significant difference occurs in the mass yield curves for the Es isotopes for the two systems. The peak cross section of the Es mass yield curve for the ^{40}Ar system is a factor of 3.5 higher than the peak from the ^{44}Ca system. This difference might possibly be due to the calculated excitation energies being more negative for the ^{44}Ca system than for the ^{40}Ar system. The width of the Es peak from the ^{40}Ar is much narrower than the peak from the ^{44}Ca with FWHM's of 1.5 and 2 mass units respectively. The yields for the neutron-rich Es isotopes are also larger for the ^{40}Ar system.

The isotopic distributions for the Fm isotopes have similar shapes for the 2 systems. However, the FWHM's cannot be determined for these curves because of the absence of data for the the neutron-deficient Fm isotopes. Once again the ^{40}Ar system has larger cross sections for the neutron-rich Fm isotopes.

3. Comparison of the ^{40}Ar system with other heavy ion systems

The peaks of the mass distributions for various projectiles on ^{248}Cm targets are shown in Table I. For the Bk curves, four of the six peaks occur at ^{248m}Bk. However, for ^{18}O and ^{132}Xe the maxima occur at ^{250}Bk and ^{249}Bk respectively. As stated in Section A.2, the peaks of the distributions should occur at the nuclide which results from the fewest number of nucleons transferred for which E_x is positive. For the Bk isotopes, ^{249}Bk requires the transfer of only one nucleon, hence if E_x is positive for this nuclide the peak should occur here. E_x is positive for the ^{40}Ca, ^{44}Ca, and ^{40}Ar systems for ^{249}Bk. For these systems, cross sections were not measured for ^{249}Bk; however, from the systematics of the cross sections of the other

Bk isotopes it was determined that the peaks occur at ^{248m}Bk for these systems. E_x is slightly negative for the ^{18}O and ^{132}Xe systems so one would not expect the maxima to be at ^{249}Bk for these systems.

In five out of the six cases, the maxima of the Cf distributions occur at ^{250}Cf, the Cf isotope which results from the transfer of the fewest possible number of nucleons. ^{40}Ca is the exception with the maximum occurring at ^{248}Cf. E_x is positive for ^{250}Cf for the ^{40}Ca, ^{44}Ca, ^{40}Ar, ^{18}O, and ^{132}Xe systems. However, it is negative for the ^{48}Ca system as are all of the E_x's for the Cf isotopes produced in the ^{48}Ca system.

^{251}Es, the Es isotope produced from the transfer of the fewest number of nucleons, is the maximum for the ^{44}Ca, ^{40}Ar, and ^{132}Xe systems. E_x is positive for these except in the case of ^{132}Xe where it is only -0.02. Since the E_x's are based upon mass excess values their accuracy cannot be expected to be better than 0.5 MeV. For the ^{40}Ca system the E_x's are all positive and the maximum occurs at ^{250}Es. For the ^{18}O system, however, the maximum occurs at ^{253}Es which in this case corresponds to the nuclide which has the fewest number of nucleons transferred for which E_x is positive. The ^{48}Ca system, which has negative E_x's for all of the Es isotopes, has its maximum at ^{253}Es.

The fewest number of nucleons which can be transferred in order to make a Fm isotope is four protons, which would produce ^{252}Fm. Due to insufficient data as stated in C.1, the peaks of the mass distribution for the ^{44}Ca and the ^{40}Ar systems for the Fm isotopes cannot be located. However, in both cases, E_x's are positive for ^{252}Fm. The peak of the ^{40}Ca system, with all positive E_x values, is ^{251}Fm. The peak of the mass distribution for the ^{18}O system occurs at ^{254}Fm. Again, this is the nuclide resulting from the transfer of the fewest number of nucleons for which E_x is positive. In the ^{48}Ca system, where the E_x values are all negative, the maximum is at ^{255}Fm. Finally, ^{132}Xe has its maximum at ^{253}Fm with an E_x of 0.20.

IV. SUMMARY

From the results of this study the following conclusions can be made:

1. The cross sections generally decrease as the number of nucleons transferred increases.

2. The shapes of the excitation functions for the ^{40}Ar and ^{44}Ca systems are consistent with their calculated excitation energies.

3. For both the ^{40}Ar and ^{44}Ca systems, the maxima of the isotopic distributions generally occur for those reaction channels which involve the apparent exchange of the fewest number of nucleons for which E_x is a positive quantity. The maxima of the isotopic distributions of the ^{40}Ca system, however, are an exception to this behavior. Deviations such as these indicate that factors other than E_x might also be influencing the final production cross section distributions such as Z/A equilibration.

4. ^{40}Ar, which is more neutron-rich than ^{44}Ca, enhances the production of neutron-rich actinide products relative to ^{44}Ca. This is in agreement with previous studies in which it was shown that the neutron-rich projectiles enhance the formation of neutron-rich actinide products.

5. It appears that most of the data can be explained by a binary-type transfer mechanism in which the projectile transfers relatively little excitation energy to the target-like product.

ACKNOWLEDGMENTS

This work was supported in part by the Director, Office of Energy Research, Division of Nuclear Physics of the Office of High Energy and Nuclear Physics of the U.S. Department of Energy under Contract No. DE-AC03-76SF00098.

The authors wish to thank the staff and crew of the LBL 88-Inch Cyclotron for their assistance.

The authors are indebted for the use of the ^{248}Cm to the Division of Chemical Sciences, Office of Basic Energy Sciences, U.S. Department of Energy, through the transplutonium element production facilities at the Oak Ridge National Laboratory.

The authors wish to thank Elizabeth Brady for her assistance in preparation of this manuscript.

REFERENCES

1. R. Kaufman and R. Wolfgang, Phys. Rev. 121, 192 (1960).

2. D.C. Hoffman, Americium and Curium Chemistry and Technology, 241-250 (1985).

3. D.C. Hoffman, M.M. Fowler, W.R. Daniels, H.R. von Gunten, D. Lee, K.J. Moody, K. Gregorich, R. Welch, G.T. Seaborg, W. Brüchle, M. Brügger, H. Gäggeler, M. Schädel, K. Sümmerer, G. Wirth, Th. Blaich, G. Herrmann, N. Hildebrand, J.V. Kratz, M. Lerch, and N. Trautmann, Phys. Rev. C 31, 1763 (1985).

4. J.D. Leyba, D.A. Bennett, R.B. Chadwick, R.M. Chasteler, C.M. Gannett, H.L. Hall, R.A Henderson, K.E Gregorich, M.J. Nurmia, D.C. Hoffman, A. Türler, and H.R von Gunten, Lawrence Berkeley Laboratory Nuclear Science Divsion Annual Report 1986-87, Report No. LBL-2529 (1988).

5. H. Gäggler, W. Brüchle, M. Brügger, M. Schädel, K. Sümmerer, G. Wirth, J.V. Kratz, M. Lerch, Th. Blaich, G. Herrmann, N. Hildebrand, N. Trautmann, D. Lee, K.J. Moody, K.E. Gregorich, R.B. Welch, G.T. Seaborg, D.C. Hoffman, W.R Daniels, M.M. Fowler, and H.R. von Gunten, Phys. Rev. C 33, 1983 (1986).

6. D. Lee, H.R. von Gunten, B. Jacak, M. Nurmia, Y. Liu, C. Luo, G.T. Seaborg, and D.C. Hoffman, Phys. Rev. C 25, 286 (1982).

7. R. Welch, K.J. Moody, K.E. Gregorich, D.M. Lee, and G.T. Seaborg, Phys. Rev. C 35, 204 (1987).

8. M. Schädel, W. Brüchle, H. Gäggeler, J.V. Kratz, K. Sümmerer, G. Wirth, G. Herrmann, R. Stakemann, G. Tittel, N. Trautmann, J.M. Nitschke, E.K. Hulet, R.W. Lougheed, R.L. Hahn, and R.L. Ferguson, Phys. Rev. Lett. 48, 852 (1982).

9. D. Lee, K.J. Moody, M.J. Nurmia, G.T. Seaborg, H.R. von Gunten, and D.C. Hoffman, Phys. Rev. C 27, 2656 (1983).

10. K. Moody, D. Lee, R.B. Welch, K.E. Gregorich. G.T. Seaborg R.W. Lougheed, and E.K. Hulet, Phys. Rev. C 33, 1315 (1986).

11. P. Eskola, "Studies of Production and Decay of Some Alpha-Active Isotopes of Einsteinium, Mendelevium, Nobelium and

Lawrencium," Dept. of Physics, University of Helsinki, Report Series in Physics 195, No. D5 (1975).

12. F. Mylius and C. Hüttner, Bec. Deut. Chem. Ges. 44, 1315 (1911).

13. J.T. Routti, and S.G. Prussin, Nucl. Inst. Meth. 72, 125 (1969).

14. K.E. Gregorich, Ph.D. Thesis, LBL-20192.

15. J.B. Cumming, NAS-NS 3107, 25 (1963).

16. D.C. Hoffman and M.M. Hoffman, Los Alamos National Laboratory Report LA-UR-82-824, March 1982.

17. H.C. Britt, in Proceedings of the Forth International Atomic Energy Agency Symposium on Physics and Chemistry of Fission, Jülich, 1979, (IAEA, Vienna, 1980), Vol. I, p. 3.

18. H.C. Britt, E. Cheifetz, D.C. Hoffman, J.B. Wilhelmy, R. J. Dupzyk, and R.W. Lougheed, Phys. Rev. C 21, 761 1980.

19. J.D. Leyba unpublished data.

Table I. Neutron to proton ratios and peaks of mass distributions for various projectiles on ^{248}Cm targets.

Projectile	N/Z	Peak of Mass Distributions			
		Bk	Cf	Es	Fm
^{40}Ca	1.00	248	248	250	251
^{44}Ca	1.20	248	250	251	≤252
^{40}Ar	1.22	248	250	251	≤252
^{18}O	1.25	250	250	253	254
^{48}Ca	1.40	248	250	252	255
^{132}Xe	1.44	249	250	251	253

Table II. Cross sections from bombardments of ^{248}Cm with ^{40}Ar.

Nuclide	207 MeV Cross Section (μb)	207 MeV s (%)	225 MeV Cross Section (μb)	225 MeV s (%)	245 MeV Cross Section (μb)	245 MeV s (%)	266 MeV Cross Section (μb)	266 MeV s (%)	286 MeV Cross Section (μb)	286 MeV s (%)
Bk 244	4.20	20	14.5	2.7	19.5	4.7	8.53	11	6.62	5.2
245	84.8	4.5	299	2.0	414	2.3	293	1.9	126	2.7
246	342	1.3	1115	1.3	1400	1.5	1115	21	540	5.6
248m	907	6.0	3080	11.3	4210	11	3900	37	2010	22
250	311	1.8	1080	1.4	1670	1.7	1660	1.3	1200	1.5
251	64.8	3.9	27.5	7.9	350	25	240	15	100	11
Cf 246	19.2	0.6	64.0	0.4	77.2	0.5	69.0	0.3	3.26	4.9
248	449	0.9	1320	0.6	1630	0.4	1560	0.7	925	0.3
250	2100	0.7	5160	0.5	5920	0.7	7600	0.5	3970	0.6
252	301	0.9	755	0.7	955	0.8	852	3.5	303	6.9
253	4.58	1.8	15.7	1.2	17.1	1.5	14.9	1.5	7.07	1.7
254	0.46	3.8	1.22	2.9	1.42	3.6	1.16	3.2	0.48	4.5
Es 250	54.0	15	127	65	230	10	81.0	22	25.0	18
251	17.0	15	472	3.5	900	15	430	26	150	20
252	76.3	7.9	179	6.2	287	21	74.9	22	19.5	50
253	17.5	1.9	37.7	1.7	41.6	8.3	17.1	5.5	7.5	12
254m	1.19	1.9	3.63	1.3	4.04	2.1	1.36	2.3	0.56	3.5
255	0.07	14	0.11	25	0.23	18	0.16	19	0.03	54
Fm 252	7.19	8.6	18.4	5.0	16.4	5.1	7.71	7.2	2.28	1.9
253	6.58	9.9	16.8	0.8	9.70	9.6	5.20	6.0	2.29	5.7
254	6.14	1.8	6.58	1.4	5.18	2.9	2.55	4.2	0.73	5.6
255	2.40	23	4.43	3.2	3.41	25	0.89	63	0.42	51
256	0.34	4.9	0.46	3.3	0.59	6.6	0.19	12	0.03	21

Table III. Calculated excitation energies for above target actinide products for reactions of ^{40}Ar with ^{248}Cm. M is the total number of nucleons transferred.

Nuclide	M	E_x (MeV)	Nuclide	M	E_x (MeV)
^{244}Bk	6	0.05	^{246}Cf	6	1.72
^{245}Bk	5	3.01	^{247}Cf	5	1.35
^{246}Bk	4	1.26	^{248}Cf	4	4.16
^{247}Bk	3	2.92	^{249}Cf	3	2.10
^{248}Bk	2	-0.16	^{250}Cf	2	4.16
^{249}Bk	1	0.24	^{251}Cf	3	0.88
^{250}Bk	2	-3.23	^{252}Cf	4	2.37
^{251}Bk	3	-3.16	^{253}Cf	5	-3.12
			^{254}Cf	6	-4.47
^{249}Es	5	-1.26	^{251}Fm	5	-3.08
^{250}Es	4	-1.36	^{252}Fm	4	1.42
^{251}Es	3	1.39	^{253}Fm	5	0.88
^{252}Es	4	0.04	^{254}Fm	6	4.18
^{253}Es	5	2.10	^{255}Fm	7	1.23
^{254}Es	6	-1.67	^{256}Fm	8	2.69
^{255}Es	7	-2.28			
^{256}Es	8	-7.84			

Table IV. Calculated excitation energies for above target actinide products for reactions of ^{44}Ca with ^{248}Cm. M is the total number of nucleons transferred.

Nuclide	M	E_x (MeV)	Nuclide	M	E_x (MeV)
^{244}Bk	6	6.76	^{246}Cf	6	8.39
^{245}Bk	5	8.78	^{247}Cf	5	5.93
^{246}Bk	4	5.50	^{248}Cf	4	7.16
^{247}Bk	3	5.39	^{249}Cf	3	4.07
^{248}Bk	2	1.38	^{250}Cf	2	4.72
^{249}Bk	1	0.32	^{251}Cf	3	0.06
^{250}Bk	2	-4.70	^{252}Cf	4	-0.23
^{251}Bk	3	-6.03	^{253}Cf	5	-5.67
			^{254}Cf	6	-6.61
^{249}Es	5	2.26	^{251}Fm	5	0.41
^{250}Es	4	1.19	^{252}Fm	4	3.36
^{251}Es	3	2.49	^{253}Fm	5	1.25
^{252}Es	4	-0.47	^{254}Fm	6	3.22
^{253}Es	5	-0.31	^{255}Fm	7	0.01
^{254}Es	6	-3.67	^{256}Fm	8	1.72
^{255}Es	7	-4.09			
^{256}Es	8	-9.84			

Table V. Calculated fraction of energy transferred, F_t, from ^{40}Ar projectile to ^{248}Cm target. $E_{f,n}$ is either the height of the fission barrier or the neutron binding energy in MeV whichever is lower, E_M is the maximum in the experimental excitation functions, and E_t is the fraction of energy transferred assuming it is apportioned according to the mass fraction transferred. $E_B \approx 211$ MeV in the lab frame.

Nuclide	E_M (MeV)	F_t	E_t	Nuclide	E_M (MeV)	F_t	E_t
Bk 244	240	0.21	0.15	Es 250	243	0.21	0.10
245	245	0.10	0.13	251	245	0.12	0.08
246	242	0.15	0.10	252	240	0.18	0.10
248m	250	0.15	0.05	253	237	0.13	0.13
250	255	0.19	0.05	254m	237	0.26	0.15
				255	250	0.20	0.18
Cf 246	245	0.10	0.15	Fm 252	235	0.18	0.10
248	255	0.02	0.10	253	228	0.28	0.13
250	266	0.02	0.05	254	220	0.17	0.15
252	245	0.08	0.10	255	230	0.21	0.18
253	245	0.23	0.13	256	245	0.09	0.20
254	245	0.29	0.15				

Table VI. Calculated fraction of energy transferred, F_t, from ^{44}Ca projectile to ^{248}Cm target. $E_{f,n}$ is either the height of the fission barrier or the neutron binding energy in MeV whichever is lower, E_M is the maximum in the experimental excitation functions, and E_t is the fraction of energy transferred assuming it is apportioned according to the mass fraction transferred. $E_B \approx 237$ MeV in the lab frame. An * indicates that $(E_{f,n}-E_x)<0$. Data taken from reference 2.

Nuclide	E_M (MeV)	F_t	E_t	Nuclide	E_M (MeV)	F_t	E_t
Bk 244	285	*	0.14	Es 250	275	0.11	0.09
245	285	*	0.11	251	275	0.08	0.07
246	282	0.01	0.09	252	273	0.16	0.09
248m	286	0.08	0.05	253	266	0.20	0.11
250	≥319	≤0.01	0.05	254m	273	0.24	0.14
				255	252	0.63	0.16
Cf 246	275	*	0.14	Fm 252	252	0.16	0.09
247	275	*	0.11	253	264	0.16	0.11
248	275	*	0.09	254	256	0.13	0.14
250	260	0.21	0.05	256	252	0.26	0.18
252	280	0.13	0.09				
253	270	0.32	0.11				
254	292	0.21	0.14				

FIGURE CAPTIONS

Figure 1 Target system schematic diagram.

Figure 2 Flow chart of the chemistry performed on Au catcher foils.

Figure 3 Excitation functions for isotopes of Bk from the reactions of ^{40}Ar with ^{248}Cm.

Figure 4 Excitation functions for isotopes of Cf from the reactions of ^{40}Ar with ^{248}Cm.

Figure 5 Excitation functions for isotopes of Es from the reactions of ^{40}Ar with ^{248}Cm.

Figure 6 Excitation functions for isotopes of Fm from the reactions of ^{40}Ar with ^{248}Cm.

Figure 7 Isotopic distributions for Bk, Cf, Es, and Fm from the interactions of 245-MeV (1.16 X Coulomb barrier) ^{40}Ar ions with ^{248}Cm.

Figure 8 Isotopic distributions for Bk, Cf, Es, and Fm from the interactions of 275-MeV (1.16 X coulomb barrier) ^{44}Ca ions with ^{248}Cm.

Figure 9 Isotopic distributions for Bk produced from the interactions of 113-MeV (1.20 X Coulomb barrier) ^{18}O ions, 245-MeV (1.16 X Coulomb barrier) ^{40}Ar ions, 253-MeV (1.08 X Coulomb barrier) ^{40}Ca ions, 275-MeV (1.16 X Coulomb barrier) ^{44}Ca ions, 280-MeV (1.19 X Coulomb barrier) ^{48}Ca ions, and 805-MeV (1.13 X Coulomb barrier) ^{132}Xe ions with ^{248}Cm.

Figure 10 Isotopic distributions for Cf produced from the interactions of 113-MeV (1.20 X Coulomb barrier) ^{18}O ions, 245-MeV (1.16 X Coulomb barrier) ^{40}Ar ions, 253-MeV (1.08 X Coulomb barrier) ^{40}Ca ions, 275-MeV (1.16 X Coulomb barrier) ^{44}Ca ions, 280-MeV (1.19 X Coulomb barrier) ^{48}Ca ions, and 805-MeV (1.13 X Coulomb barrier) ^{132}Xe ions with ^{248}Cm.

Figure 11 Isotopic distributions for Es produced from the interactions of 113-MeV (1.20 X Coulomb barrier) ^{18}O ions, 245-MeV (1.16 X Coulomb barrier) ^{40}Ar ions, 253-MeV (1.08 X

Coulomb barrier) ^{40}Ca ions, 275-MeV (1.16 X Coulomb barrier) ^{44}Ca ions, 280-MeV (1.19 X Coulomb barrier) ^{48}Ca ions, and 805-MeV (1.13 X Coulomb barrier) ^{132}Xe ions with ^{248}Cm.

Figure 12 Isotopic distributions for Fm produced from the interactions of 113-MeV (1.20 X Coulomb barrier) ^{18}O ions, 245-MeV (1.16 X Coulomb barrier) ^{40}Ar ions, 253-MeV (1.08 X Coulomb barrier) ^{40}Ca ions, 275-MeV (1.16 X Coulomb barrier) ^{44}Ca ions, 280-MeV (1.19 X Coulomb barrier) ^{48}Ca ions, and 805-MeV (1.13 X Coulomb barrier) ^{132}Xe ions with ^{248}Cm.

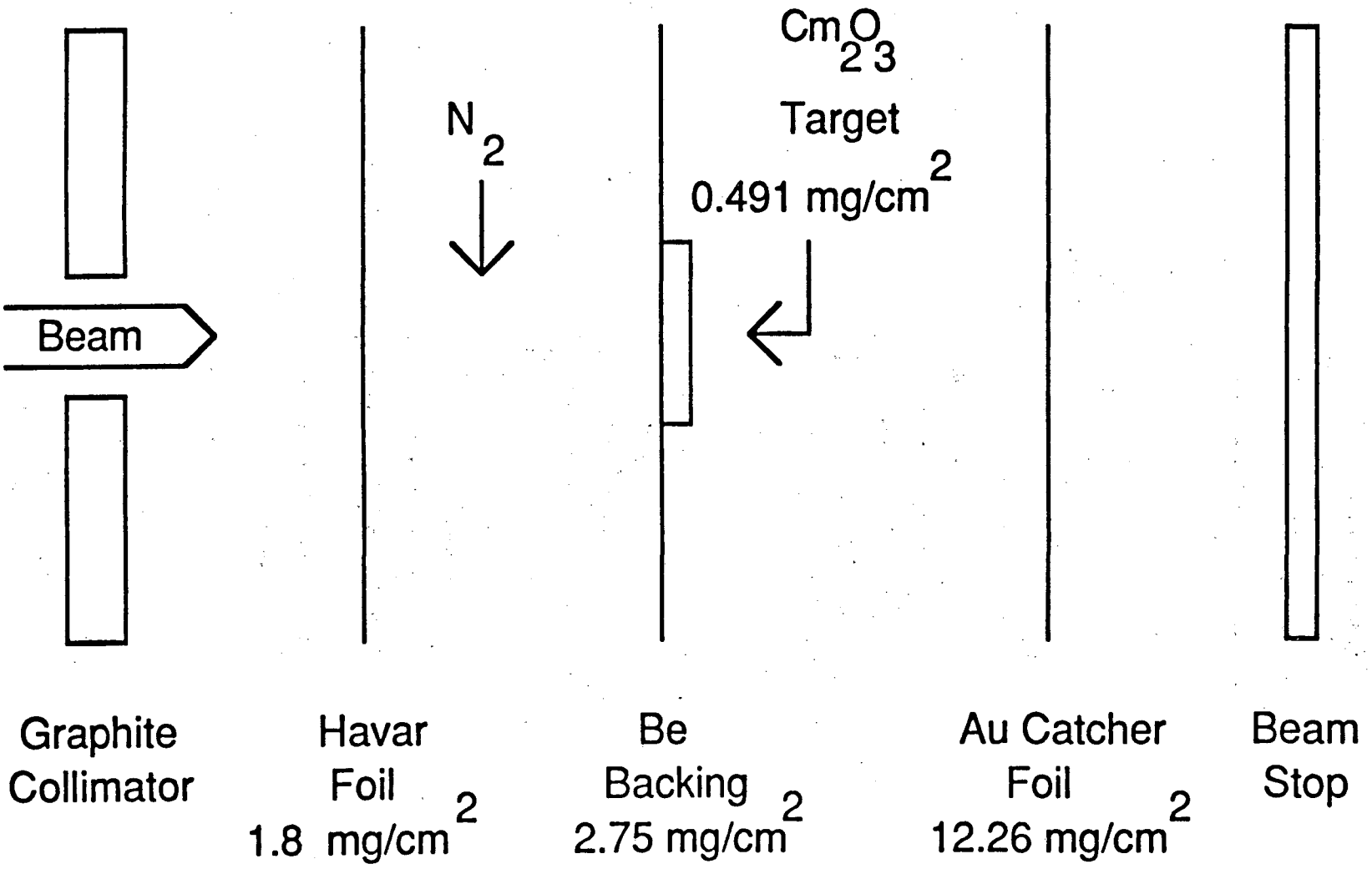
Beam
N2
Cm2O3
Target
0.491 mg/cm2
Graphite
Collimator
Havar
Foil
1.8 mg/cm2
Be
Backing
2.75 mg/cm2
Au Catcher
Foil
12.26 mg/cm2
Beam
Stop

Fig. 1
23

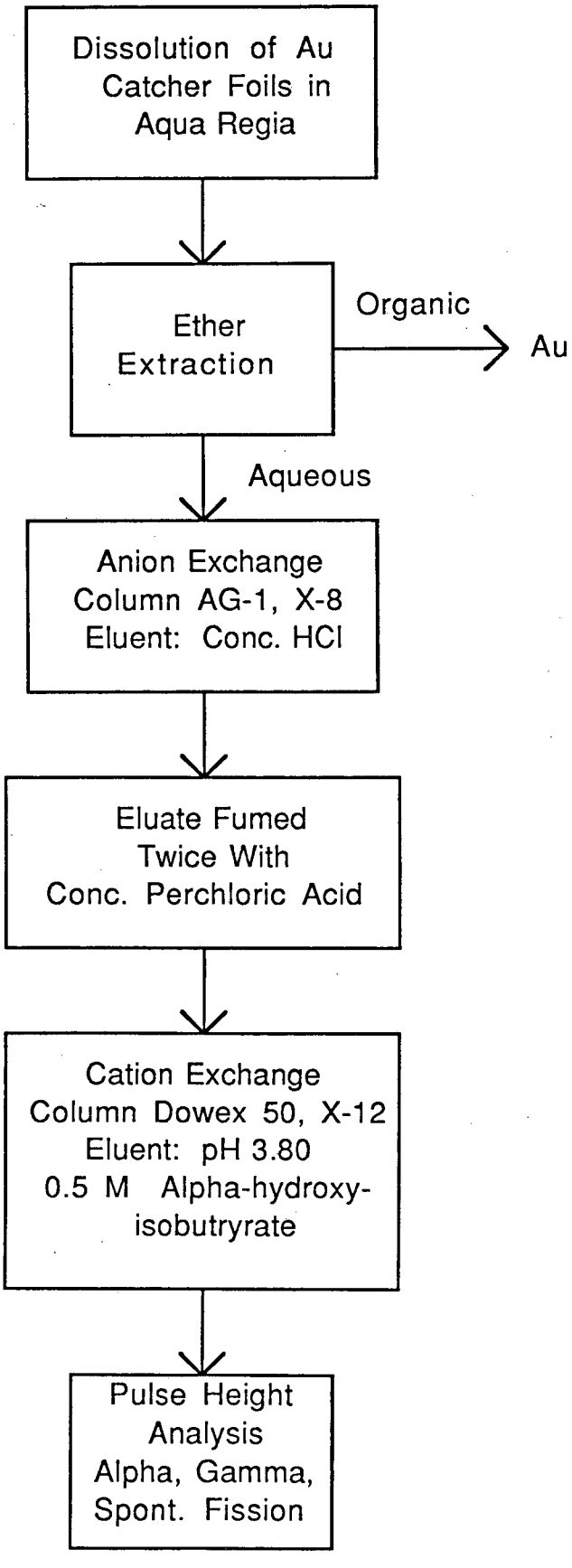
Dissolution of Au Catcher Foils in Aqua Regia
Ether Extraction
Organic
Au
Aqueous
Anion Exchange Column AG-1, X-8 Eluent: Conc. HCl
Eluate Fumed Twice With Conc. Perchloric Acid
Cation Exchange Column Dowex 50, X-12 Eluent: pH 3.80 0.5 M Alpha-hydroxy-isobutyrate
Pulse Height Analysis Alpha, Gamma, Spont. Fission

Fig. 2

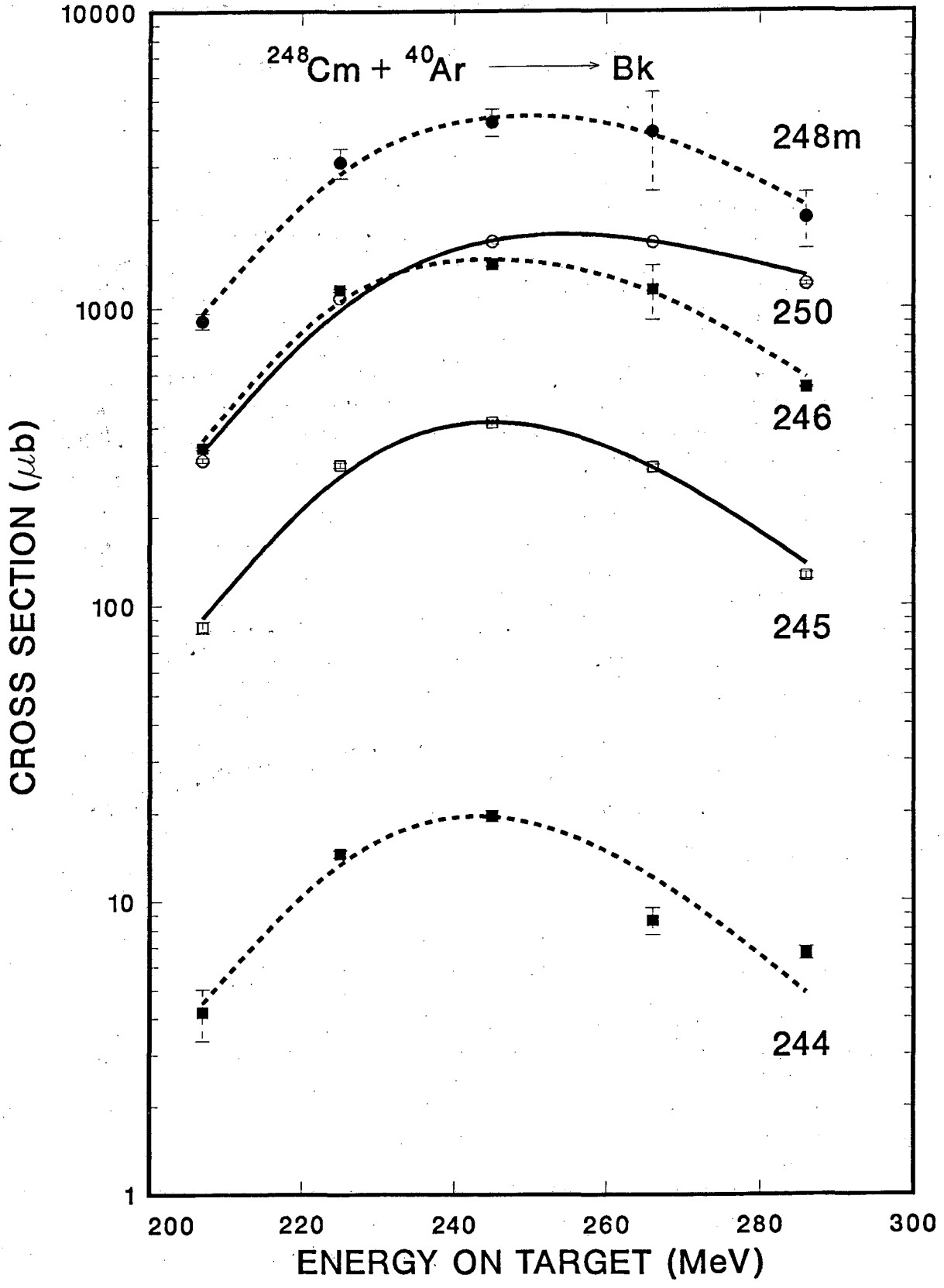
10000
1000
100
10
1
$^{248}Cm + ^{40}Ar \longrightarrow Bk$
248m
250
246
245
244
CROSS SECTION (μb)
200
220
240
260
280
300
ENERGY ON TARGET (MeV)

Fig. 3

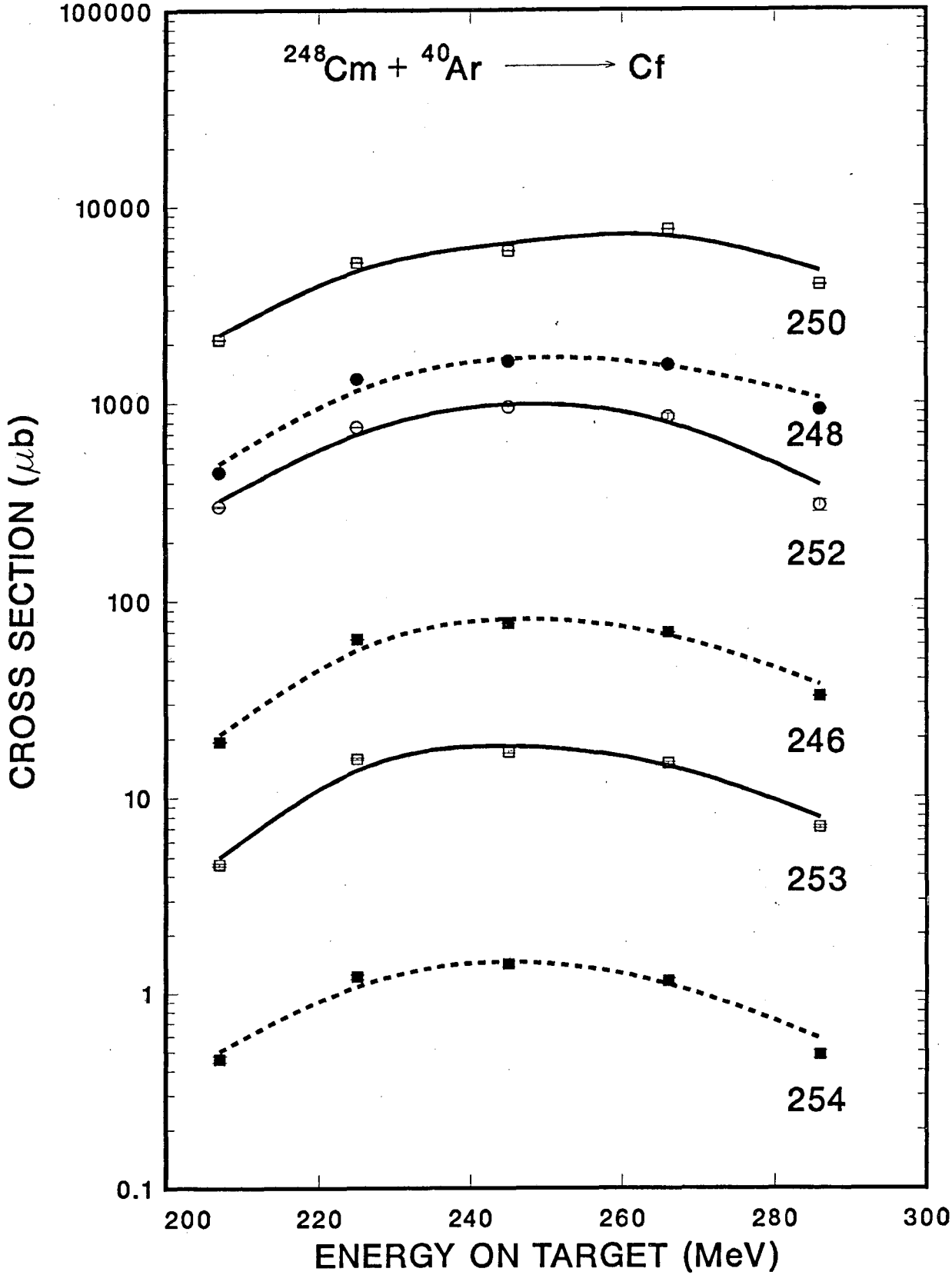
$^{248}Cm + ^{40}Ar \longrightarrow Cf$
CROSS SECTION (μb)
100000
10000
1000
100
10
1
0.1
250
248
252
246
253
254
200
220
240
260
280
300
ENERGY ON TARGET (MeV)

Fig. 4

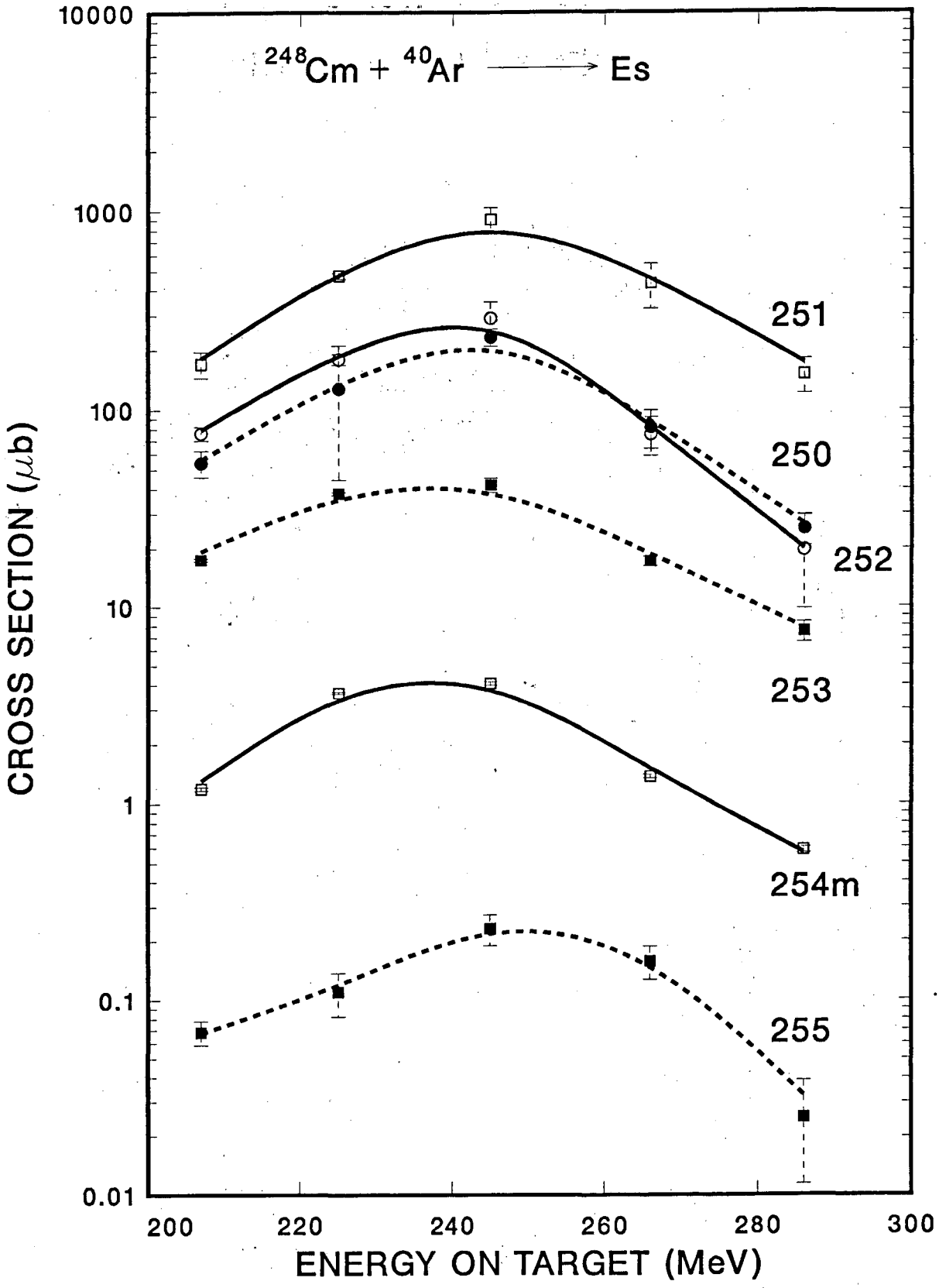
$^{248}Cm + ^{40}Ar \longrightarrow Es$
CROSS SECTION (μb)
ENERGY ON TARGET (MeV)
10000
1000
100
10
1
0.1
0.01
200
220
240
260
280
300
251
250
252
253
254m
255

Fig. 5

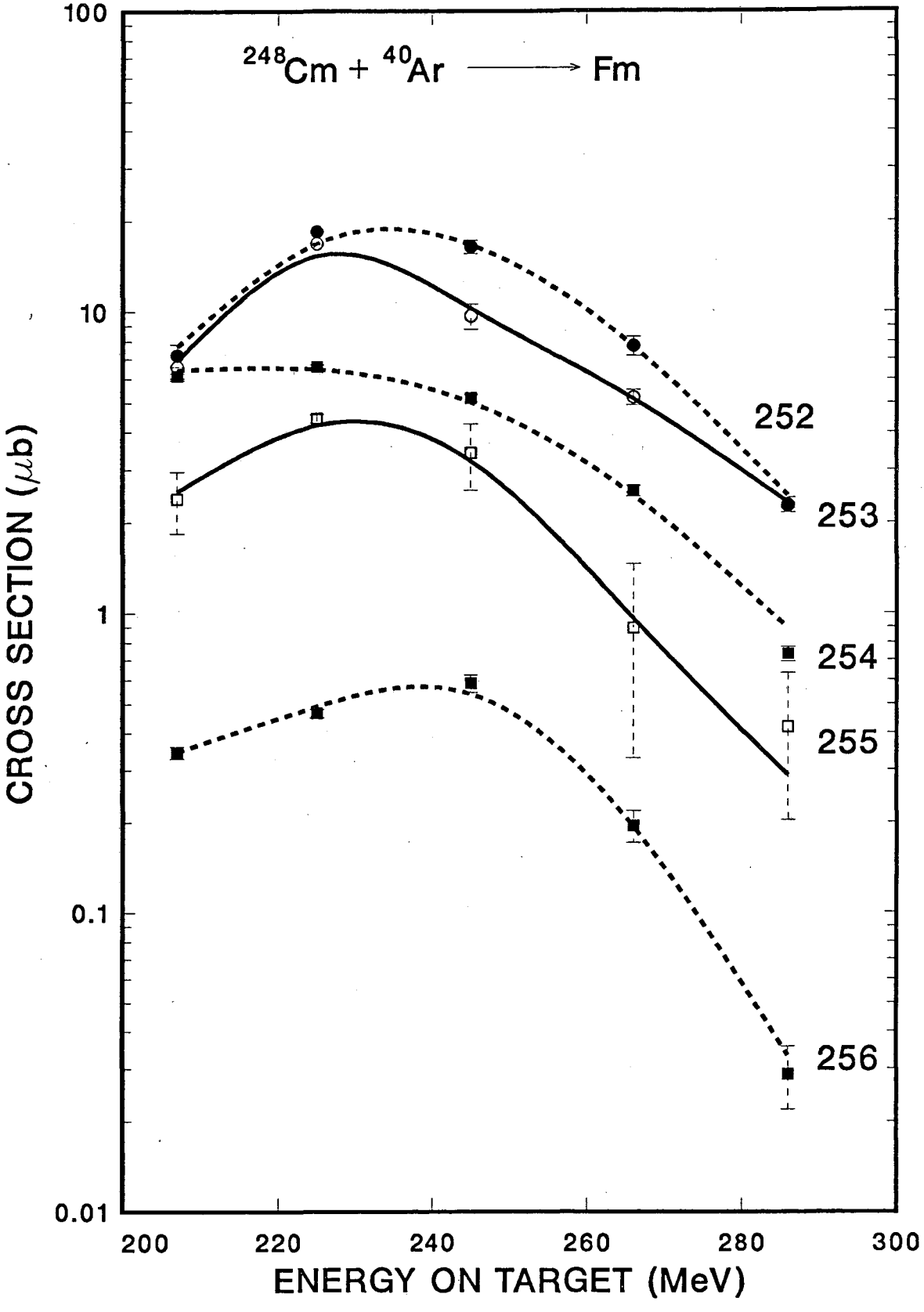
$^{248}Cm + ^{40}Ar \longrightarrow Fm$
CROSS SECTION (μb)
100
10
1
0.1
0.01
200
220
240
260
280
300
ENERGY ON TARGET (MeV)
252
253
254
255
256

Fig. 6

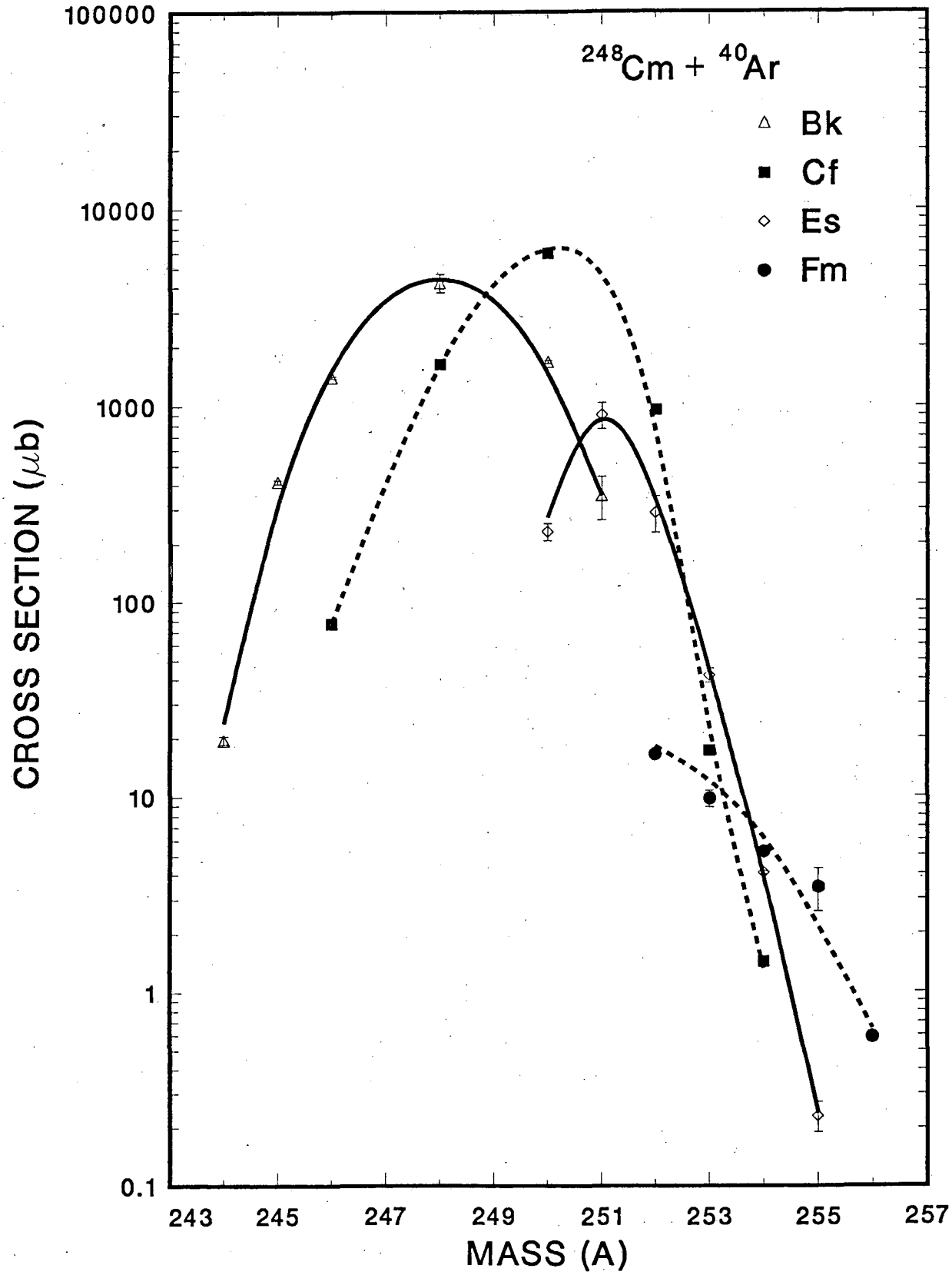
^{248}Cm + ^{40}Ar
Bk
Cf
Es
Fm
CROSS SECTION (μb)
100000
10000
1000
100
10
1
0.1
243
245
247
249
251
253
255
257
MASS (A)

Fig. 7

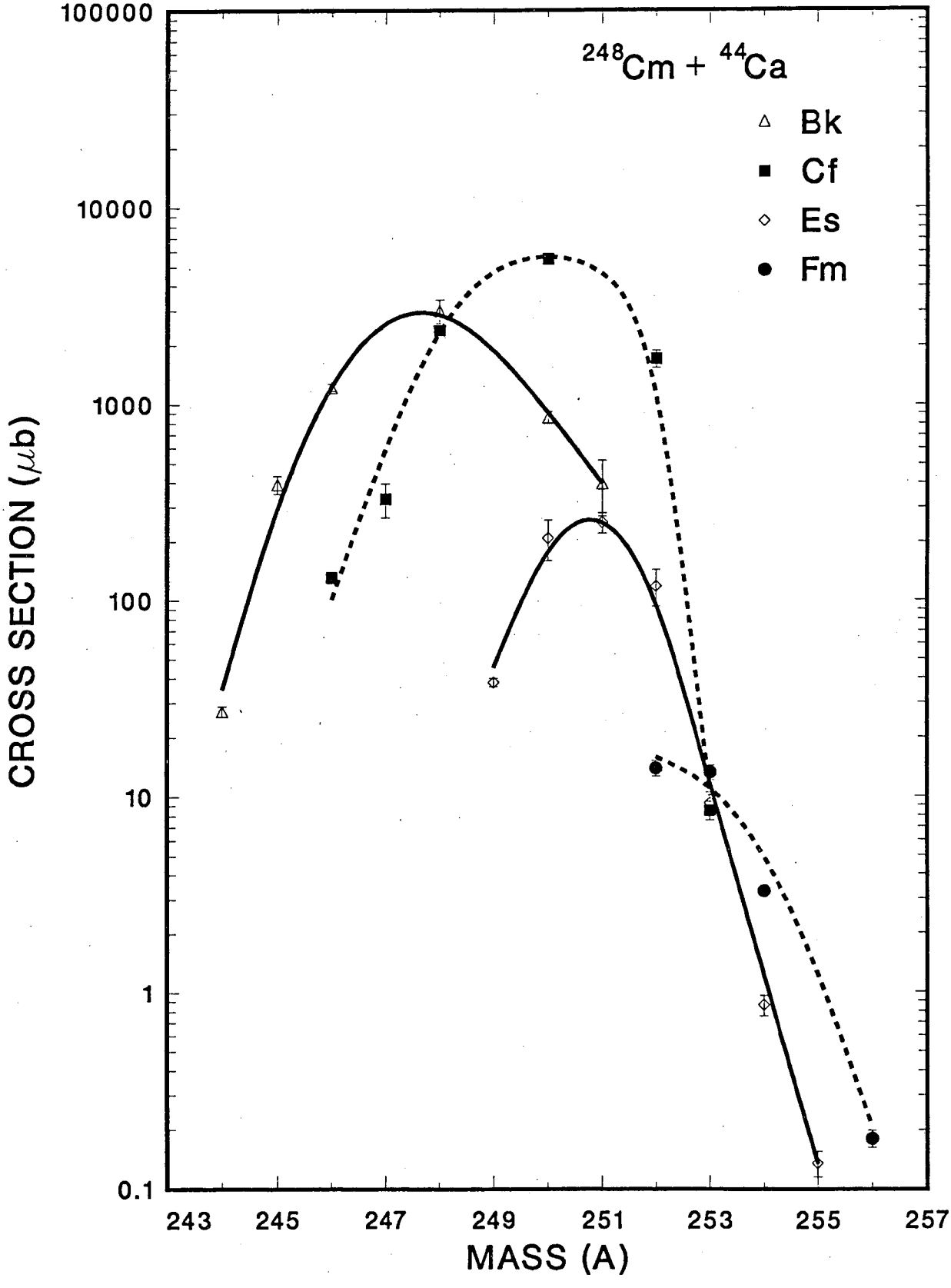
^{248}Cm + ^{44}Ca
Bk
Cf
Es
Fm
CROSS SECTION (μb)
100000
10000
1000
100
10
1
0.1
243
245
247
249
251
253
255
257
MASS (A)

Fig. 8

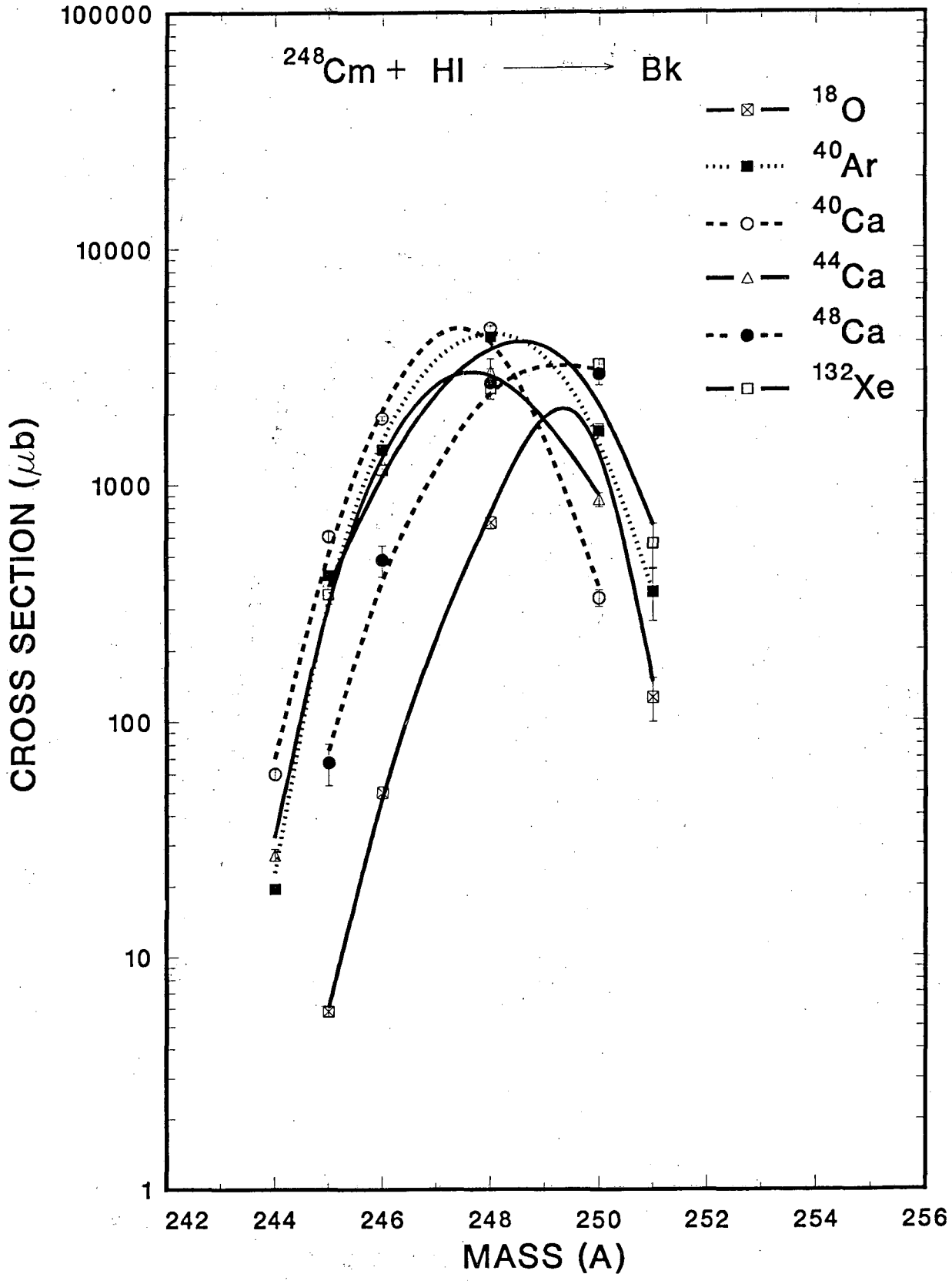
^{248}Cm + HI ⟶ Bk
^{18}O
^{40}Ar
^{40}Ca
^{44}Ca
^{48}Ca
^{132}Xe
CROSS SECTION (μb)
100000
10000
1000
100
10
1
242
244
246
248
250
252
254
256
MASS (A)

Fig. 9

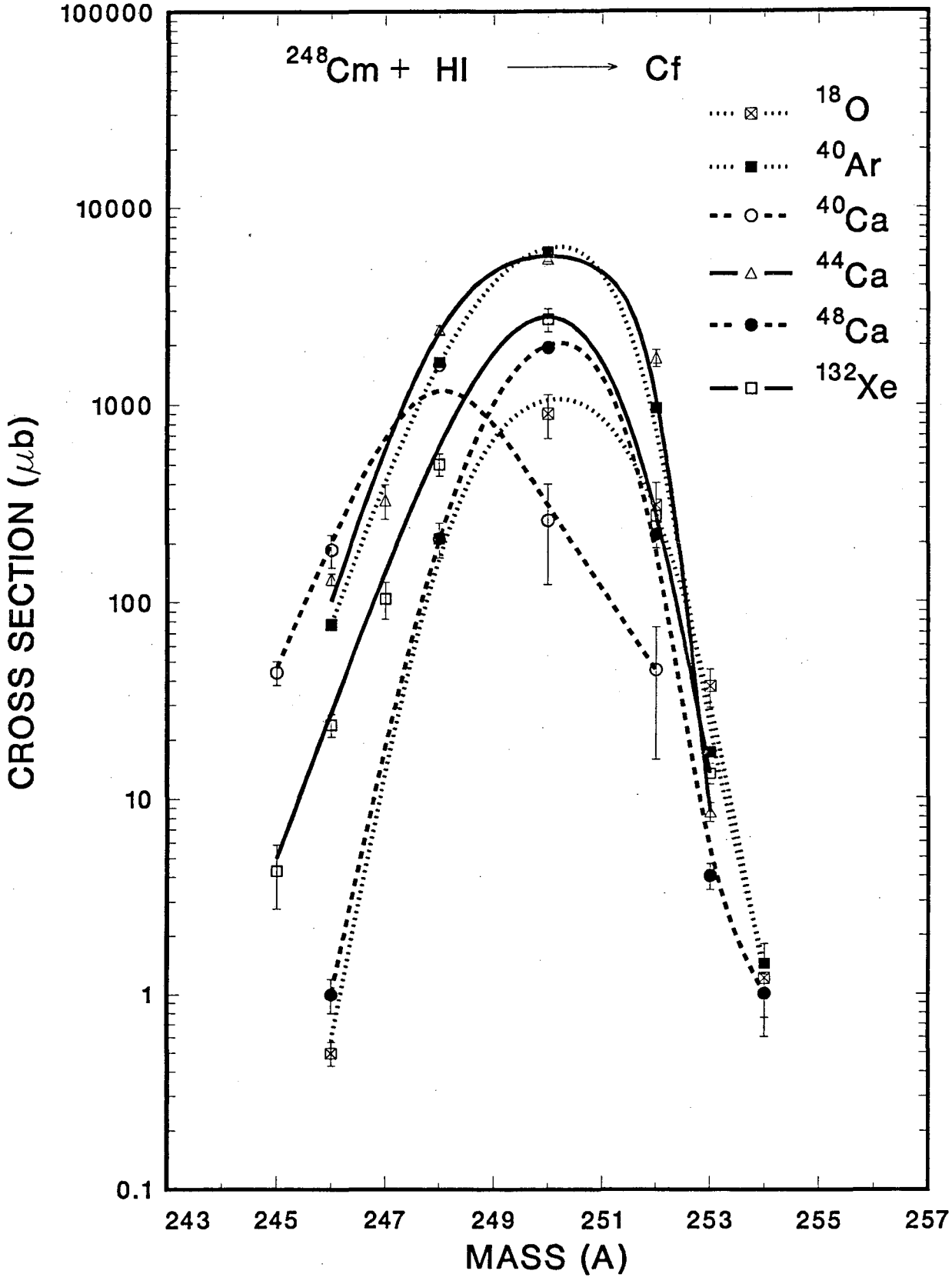
^{248}Cm + HI ⟶ Cf
^{18}O
^{40}Ar
^{40}Ca
^{44}Ca
^{48}Ca
^{132}Xe
CROSS SECTION (μb)
100000
10000
1000
100
10
1
0.1
243
245
247
249
251
253
255
257
MASS (A)

Fig. 10

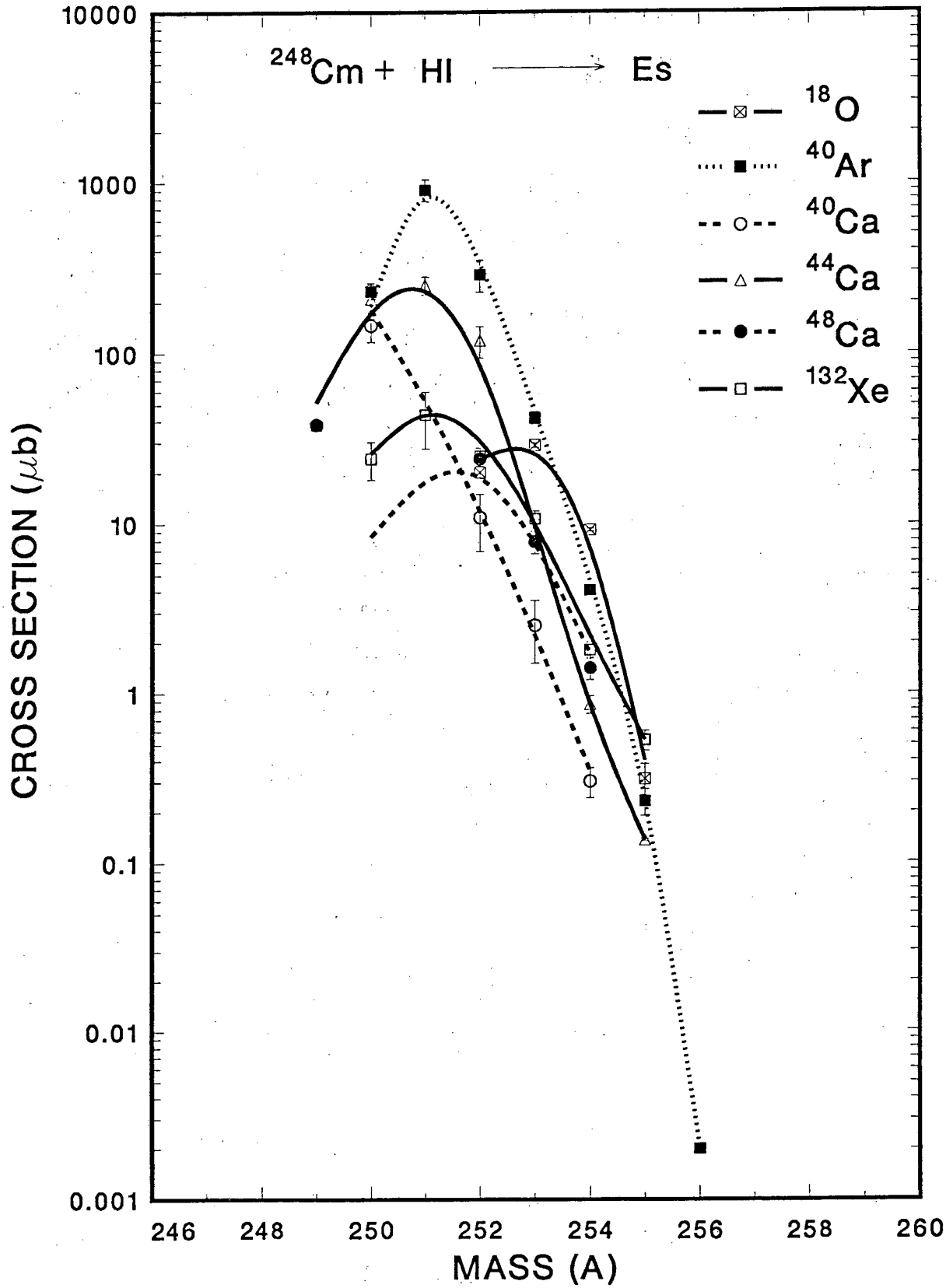
^{248}Cm + HI ⟶ Es
^{18}O
^{40}Ar
^{40}Ca
^{44}Ca
^{48}Ca
^{132}Xe
CROSS SECTION (μb)
10000
1000
100
10
1
0.1
0.01
0.001
246
248
250
252
254
256
258
260
MASS (A)

Fig. 11

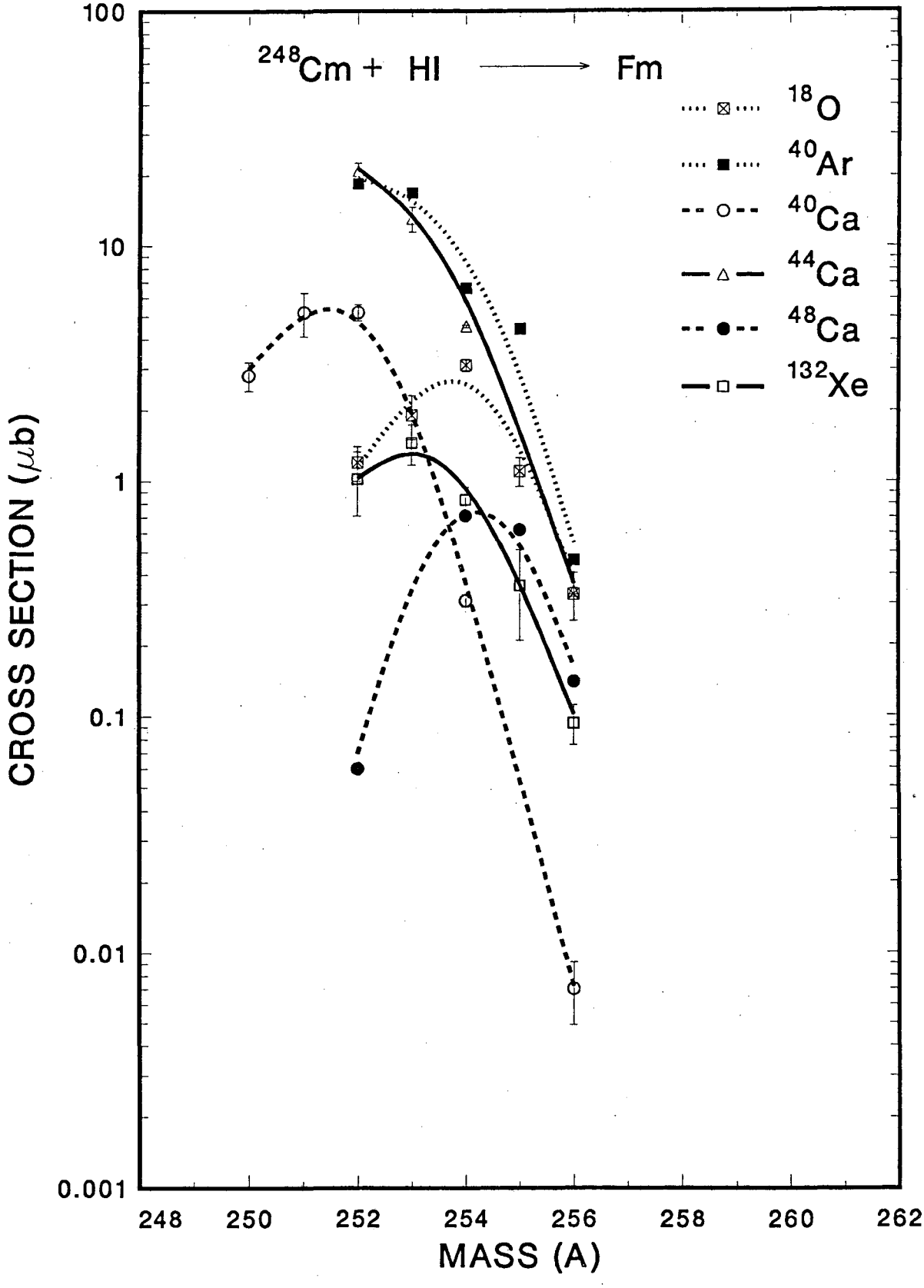
^{248}Cm + HI ⟶ Fm
^{18}O
^{40}Ar
^{40}Ca
^{44}Ca
^{48}Ca
^{132}Xe
CROSS SECTION (μb)
100
10
1
0.1
0.01
0.001
248
250
252
254
256
258
260
262
MASS (A)

Fig. 12

LAWRENCE BERKELEY LABORATORY
TECHNICAL INFORMATION DEPARTMENT
1 CYCLOTRON ROAD
BERKELEY, CALIFORNIA 94720